ARTICLE

Strong Electronic Coupling in Two-Dimensional Assemblies of Colloidal PbSe Quantum Dots

Kenrick J. Williams,[†] William A. Tisdale,[‡] Kurtis S. Leschkies,[‡] Greg Haugstad,[§] David J. Norris,[‡] Eray S. Aydil,[‡] and X.-Y. Zhu[†,*]

[†]Department of Chemistry, University of Minnesota, 207 Pleasant Street SE, Minneapolis, Minnesota 55455, [‡]Department of Chemical Engineering and Materials Science, University of Minnesota, 421 Washington Avenue SE, Minneapolis, Minnesota 55455, and [§]Institute of Technology Characterization Facility, University of Minnesota, 100 Union Street SE, Minneapolis, Minnesota 55455

ABSTRACT Thin films of colloidal PbSe quantum dots can exhibit very high carrier mobilities when the surface ligands are removed or replaced by small molecules, such as hydrazine. Charge transport in such films is governed by the electronic exchange coupling energy (β) between quantum dots. Here we show that two-dimensional quantum dot arrays assembled on a surface provide a powerful system for studying this electronic coupling. We combine optical spectroscopy with atomic force microscopy to examine the chemical, structural, and electronic changes that occur when a submonolayer of PbSe QDs is exposed to hydrazine. We find that this treatment leads to strong and tunable electronic coupling, with the β value as large as 13 meV, which is 1 order of magnitude greater than that previously achieved in 3D QD solids with the same chemical treatment. We attribute this much enhanced electronic coupling to reduced geometric frustration in 2D films. The strongly coupled quantum dot assemblies serve as both charge and energy sinks. The existence of such coupling has serious implications for electronic devices, such as photovoltaic cells, that utilize quantum dots.

KEYWORDS: nanocrystal · PbSe · quantum dot solid · two-dimensional · electronic coupling

Arrays of semiconductor quantum dots (QDs) can act as artificial solids with tunable electronic properties.[1] Such materials provide a unique model system for the study of fundamental physical processes, such as charge carrier transport, exciton diffusion, and energy transfer. To fabricate these solids, colloidal QDs are particularly attractive because their size and surface chemistry can be easily controlled.[2] Moreover, they can be processed from solution to form high quality ordered assemblies known as superlattices.[3,4] Consequently, a number of studies have explored charge transport in thin films of colloidal QDs.[5−10] However, the presence of long-chain surface ligands, which are required for the synthesis, colloidal stability, and surface passivation of the QDs, leads to poor conductivity in the films due to weak inter-QD electronic coupling. Therefore, much recent effort has focused on increasing the electronic coupling in such films to improve their conductivity.

A number of studies have explored the removal or exchange of capping molecules to increase inter-QD electronic coupling. Examples include the drying of quantum dot thin films and the partial evaporation of weakly bound capping molecules,[11,12] the chemical removal of capping molecules via reduction[13] or oxidation,[14] the thermal desorption/decomposition of capping molecules under vacuum or inert conditions,[15] and the exchange of bulky or long ligands by short ones.[16,17] A significant increase in the conductivity was demonstrated when the surface ligands were replaced by shorter molecules and charge carriers were electrochemically injected into the QDs.[16] Later it was shown that, even without the injection of extra carriers, the conductivity of films of PbSe QDs could be increased by as much as 10 orders of magnitude if films were exposed to a solution of hydrazine.[17] This dramatic increase in conductivity has been attributed to the partial removal of oleic acid ligands from the surface of the PbSe nanocrystals, resulting in decreased inter-QD spacing and increased inter-QD electronic exchange coupling. This was supported by the observation that the first exciton absorption peak shifted red by $\Delta_1 \approx$ 20 meV after immersion in 1 M hydrazine in acetonitrile. Subsequent work has examined the structural, optical, and electronic changes in PbSe QD thin films that are exposed to a variety of thermal and chemical treatments in more detail.[18,19] The observed variations included red shifts in the first exciton absorption peak of 12 and 27 meV following treatment with 1 M hydrazine in acetonitrile and in ethanol, respec-

*Address correspondence to zhu@umn.edu.

Received for review February 22, 2009 and accepted May 13, 2009.

Published online May 20, 2009.
10.1021/nn9001819 CCC: $40.75

tively. After these hydrazine treatments, it was also verified that the size of the PbSe QDs did not change, but the inter-QD distance decreased. Thus, these results support the initial claim that the red shift in the exciton transition occurs due to a decrease in the inter-QD spacing. This can cause (i) an increase in the average dielectric constant of the film, (ii) an increase in the inter-QD radiative coupling, and (iii) an increase in the inter-QD electronic coupling. However, the actual extent of the ligand exchange during the hydrazine exposure and how this impacts the accompanying optical, electronic, and structural changes is a complicated issue. Under the chemical conditions used initially (exposure to 1 M hydrazine in acetonitrile), only 2−7% of the oleic acid surface ligands are lost. A much higher percentage of ligand removal (~85−90%) of oleic acid was observed when 1 M hydrazine in ethanol solution was used instead.[18] Surprisingly, these differences in the surface coverage did not translate into dramatic changes in the conductivity. Therefore, additional experiments are needed to clarify the electronic coupling of hydrazine-treated QD solids. In particular, this would be helpful for the development of QD photovoltaic devices, for which PbSe QDs are becoming a heavily studied model system.[20,21]

To address questions about the electronic coupling, 3D QD solids may not be the best experimental system. When the surface ligands are removed from the QDs in such a film, geometric frustration may arise as the QDs try to pack more tightly or fuse. In other words, drastic structural rearrangements in the solid will be required. This can lead not only to cracks on a long length scale (>100 nm), as has been observed,[18] but also to variations in the local inter-QD spacing or the extent of aggregation and fusing. These complications due to geometric frustration can be avoided when the assembly of QDs occurs in the solution phase. Kotov and coworkers showed that, when the surface protective ligands are removed in a slow and controlled fashion, CdTe QDs in the solution can self-organize into one-dimensional pearl necklace type aggregates that subsequently recrystallize into uniform nanowires with diameters determined by those of the original QDs.[22] Fluorescence spectroscopy showed a gradual red shift of the first exciton transition by as much as ~30−60 meV in the aggregation−recrystallization process. These authors have also extended the approach to the self-assembly of CdTe QDs into free-floating two-dimensional sheets with single QD thickness.[23]

Since most applications of strongly coupled QD solids require a solid support, here we explore whether strong electronic coupling due to reduced geometric frustration is possible with chemical treatment of two-dimensional (2D) assemblies of QDs on flat surfaces. We study 2D PbSe QD solids because of the high conductivity demonstrated in this system and the extensive chemical, structural, and electronic information available from recent studies. Compared to other well-studied II−VI QD systems, such as CdSe, PbSe possesses better properties for transport. For example, it has a much higher dielectric constant (ε), lower effective masses for both the electron and the hole (m_e and m_h), and a higher density-of-states (DOS) due to a high degeneracy in the electronic energy levels.[24] High ε leads to small Coulomb charging energies (E_C) while low m_e and m_h increase the spatial extent of the electron and hole wave functions outside the QD. These factors can explain the particularly high conductivity and charge carrier mobility in films of PbSe QDs. By combining attenuated total reflection Fourier transform infrared (ATR-FTIR) spectroscopy and atomic force microscopy (AFM), we probe the chemical, structural, and electronic properties of these assemblies. We find that

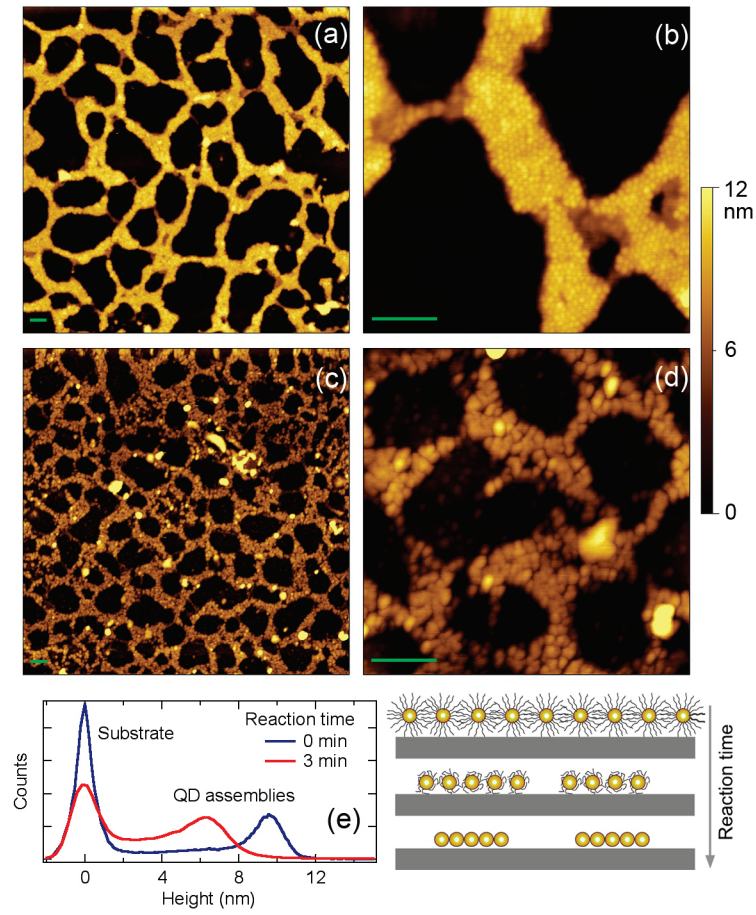

Figure 1. Attractive-regime AC-mode atomic force microscopy (AFM) images of submonolayers of PbSe QDs assembled on TiO_2(110): (a,b) as-deposited QDs with oleic acid surface ligands; (c,d) after exposure to 1 M hydrazine in acetonitrile for 3 min. Panels (b) and (d) are magnified scans of (a) and (c), respectively. All green scale bars are 100 nm. (e) Height histograms of images (a) and (c). The cartoon illustrates proposed morphology changes with reaction time. Note that the surface coverage of QDs in (a) and (c) is slightly different due to variations is the dip-coating process.

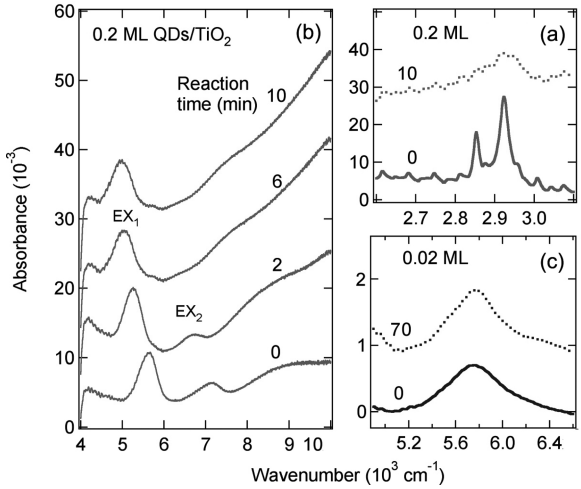

Figure 2. (a) ATR-FTIR spectra in the C−H stretch region of ~0.2 ML film of oleic-acid-capped PbSe QDs on TiO_2 before (solid line) and after (dashed line) exposure to 1 M hydrazine in acetonitrile for 10 min. (b) ATR-FTIR spectra in the exciton region (EX_1 and EX_2 label the first and second exciton transitions, respectively) of the same surface as a function of reaction time in 1 M hydrazine in acetonitrile. (c) ATR-FTIR spectra of ~0.02 ML oleic-acid-capped PbSe QDs on TiO_2 (solid) and after exposure to 1 M hydrazine in acetonitrile for 70 min (dotted line).

the electronic coupling is 10 times greater than that reported previously for 3D solids. This has implications for understanding PbSe films for transport and photovoltaic devices. Further, it demonstrates that such 2D assemblies can provide a powerful approach for studying electronic coupling in a variety of QD systems.

RESULTS AND DISCUSSION

We form 2D assemblies of PbSe QDs with oleic acid capping *via* the dip-coating method and subsequently carry out exchange reactions in 1 M hydrazine/acetonitrile solution. Figure 1 shows atomic force microscopy (AFM) images of a submonolayer of PbSe QDs on a (110) TiO_2 surface taken before and after the hydrazine exposure (3 min). Before exposure (Figure 1a), the surface is characterized by a network of two-dimensional islands. The magnified image (Figure 1b) clearly reveals hexagonally close-packed domains with an inter-QD distance of 10 ± 1 nm. This is also the height of the islands, as shown by the blue histogram in Figure 1e. The inter-QD distance and the island height are consistent with the diameter (ϕ = 6 nm ± 5%) of the QDs plus a 2 nm surface layer due to the oleic acid ligands. After hydrazine exposure, the AFM image (Figure 1c) reveals two effects. First, as shown by the red histogram in Figure 1e, the island height decreases to 6 ± 1 nm, which is identical to the size of bare QDs (*i.e.*, without their surface ligands). Second, individual QDs can no longer be resolved in the images. Both effects would be expected if the oleic acid ligands are removed and the inter-QD separation decreased. The removal of the oleic acid is also verified by vibrational spectroscopy (see below). Instead of individual QDs, the magnified image (Figure 1d) shows larger domains (lateral size 20−40 nm) that are separated by boundaries. This behavior is consistent with two-dimensional densely packed islands of QDs that suddenly lose their surface ligands while exhibiting limited mobility on the substrate. In this case, the large islands would break up into domains. Our data would then suggest that these domains correspond to 2D aggregates of 10−100 closely packed bare QDs. We estimate that the surface coverage of these 2D aggregates in our sample is ~20−30% of a monolayer (ML).

Note that, after hydrazine treatment, we also see a broadening of the height distribution (Figure 1e). This is consistent with the presence of more disorder in the 2D assemblies and the breakup of large islands as oleic acid capping molecules are removed. For small domains on the order of or smaller than the tip size, convolution of tip shape with the topography of the 2D aggregates (including some individual QDs) tends to smear out and broaden the height distribution in a topographical AFM image.

Additional information can be obtained from ATR-FTIR spectra on similar films. The hydrazine exposure induces two major changes. First, the C−H stretch at ~2920 cm^{-1} (362 meV) disappears (Figure 2a), consistent with removal of oleic acid. The residual and poorly resolved C−H stretch that remains may be attributed to background contaminants, as it is also present in the spectrum from a clean TiO_2 surface. Second, a systematic red shift in the first exciton peak with increasing hydrazine exposure time is observed (Figure 2b). For ~0.2 ML of 6 nm PbSe QDs on TiO_2, this peak shifts from 5650 (700 meV) to 5000 cm^{-1} (620 meV) after 10 min of exposure to 1 M hydrazine in acetonitrile. This shift is independent of the nature of the substrate surface, as a nearly identical shift is observed for the same coverage of PbSe QDs assembled on the SiO_2-terminated Si surface. However, the red shift is not observed when the starting coverage of PbSe QDs is significantly lower, as shown in Figure 2c for 0.02 ML after hydrazine expo-

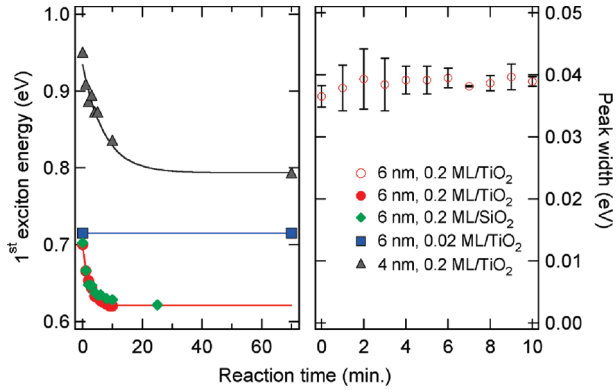

Figure 3. Right: Width of the first exciton absorption peak as a function of the exposure time to 1 M hydrazine for 0.2 ML of 6 nm QDs on TiO_2. Left: Energy of the first exciton transition as a function of the exposure time to 1 M hydrazine in acetonitrile for the indicated surface coverage and QD diameter (red, 0.2 ML of 6 nm QDs; blue, 0.02 ML of 6 nm QD; gray, 0.2 ML of 4 nm QDs) on SiO_2 (green) and TiO_2 (all other colors).

sure for 70 min. Finally, the magnitude of the red shift depends on the size of the QDs. For smaller QDs of ϕ = 4 nm, the maximum red shift is almost twice as large as that of ϕ = 6 nm. Note that hydrazine treatment of the 0.2 ML samples also increases the absorbance at energies higher than the first exciton transition (Figure 2b). This has been observed before for multilayer PdSe thin films and was attributed to enhanced electronic exchange coupling between QDs,[18,19] although changes in light scattering may also play a role.

The left panel in Figure 3 summarizes the observed shift of the first exciton transition energy as a function of reaction time for ~0.2 ML of 4 nm QDs on TiO_2 (gray triangles), ~0.2 ML of 6 nm QDs (red circles on TiO_2 and green diamonds on SiO_2-terminated silicon), and ~0.02 ML of 6 nm QDs on SiO_2 (squares). For the low surface coverage (0.02 ML), the exciton transition energy does not change with hydrazine exposure time. For the high surface coverages (0.2 ML), the exciton transition energy as a function of exposure time can be described well by an exponential decay (solid curves) for both sizes and most of the shifts occur within the first 10 min of reaction time. In contrast to peak position, width of the first exciton absorption peak increases only slightly following hydrazine treatment (≤10% increase), as shown in the right panel for 6 nm PbSe QDs.

For comparison, the red shift in the first exciton transition energy is much smaller when the thickness of the QD film is more than one monolayer. Figure 4 shows FTIR spectra of a 20 nm thick film of PbSe QDs (diameter slightly less than 6 nm) deposited on the SiO_2 surface. With increasing time of hydrazine exposure, we see up to 80% loss of oleic acid ligands for a total reaction time of 60 min (left panel). The first exciton transition red shifts by a total of 204 cm^{-1} (25 meV), right panel. This red shift is a factor of 3−4 smaller than that for the submonolayer coverage.

Three possible explanations exist for the much larger red shift in the first exciton transition upon exposure to hydrazine for monolayer QDs than that for multilayers: (i) growth in the size of the QDs, (ii) an increase in electronic interactions between the QDs and the substrate, or (iii) an increase in inter-QD electronic coupling. The first possibility can be eliminated for the following reasons. The PbSe QDs used in this study had a narrow size distribution (±5%). Growth of some PbSe QDs can only occur if others in the distribution shrink. This ripening of the distribution would lead to a broadening of the exciton transition, rather than a systematic red shift. Growth of the PbSe QDs is also unlikely since the height of the films after hydrazine exposure (Figure 1e) quantitatively matched what would be expected for our bare QDs. (A similar conclusion was reached by Nozik and coworkers during their detailed studies on the influence of hydrazine on PbSe QDs.) The second explanation can also be eliminated as the systematic red shift was observed for 2D PbSe QD assemblies not only on TiO_2 but also on SiO_2, which has a much wider band gap. Both the electron and hole levels of the PbSe QDs would be located in the band gap of SiO_2. Thus, strong electronic coupling would not be expected. In contrast, an increase in the inter-QD electronic coupling can explain all of our observations. In this case, the red shift results when the QDs move closer to each other after hydrazine exposure and 2D aggregates form. This conclusion is consistent with (i) the disappearance of the oleic acid in ATR-FTIR spectroscopy, (ii) the inability to resolve individual QDs in AFM, (iii) the decrease in island height from 10 to 6 nm, and (iv) the absence of a red shift at very low surface coverages when the adsorbed QDs are isolated. There are two ways to understand the increased inter-QD electronic coupling.

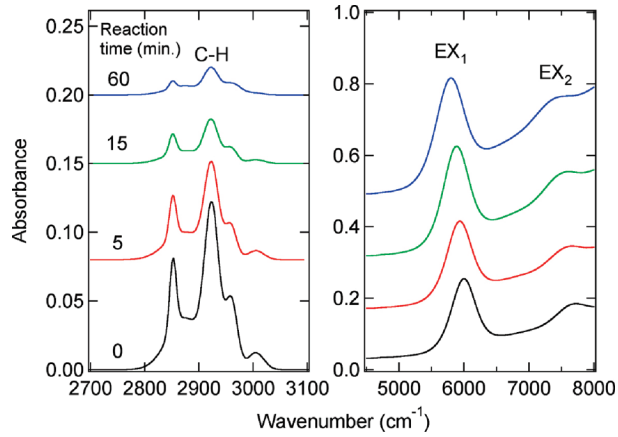

Figure 4. ATR-FTIR spectra for a 20 nm thick film of oleic-acid-capped PbSe QDs (~6 nm diameter) on SiO_2 as a function exposure time to 1 M hydrazine in acetonitrile for 0−60 min.

The first picture considers the uniform decrease of inter-QD separation as capping molecules are removed and the molecular capping layer gets thinner. With decreasing inter-QD separation, the electronic exchange coupling energy, $\beta = \langle a|\hat{H}|b\rangle$ (between two neighboring quantum dots *a* and *b*), would be expected to increase due to more spatial overlap of the wave functions. This would lead to a red shift in the first exciton transition, as illustrated in Figure 5. In particular, for a hexagonally close-packed 2D assembly of s-orbitals, tight-binding theory predicts that a new electronic band would form

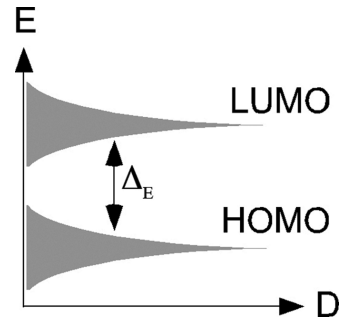

Figure 5. Schematic illustration of band formation in a QD solid as the inter-QD distance (*D*) decreases; Δ_E is the exciton transition energy.

with an energy width of 12|β|.[25] If such a band is formed both by the 1s electron and hole levels of the QDs, we can estimate the first exciton transition energy (Δ_E) at a particular interparticle separation D as

$$\Delta_E = \Delta_E^0 - (6|\beta_e| + 6|\beta_h|) \approx \Delta_E^0 - 12|\beta| \quad (1)$$

where Δ_E^0 is the first exciton transition energy for isolated QDs, and β_e and β_h are the electronic exchange coupling energies for the electron and hole levels, respectively. Equation 1 neglects the exciton binding energy and assumes that β_e and β_h are close in value. The latter is justified since m_e and m_h in PbSe are very similar.[24] With this simple model, the red shift can be estimated to be 12|β|. Note that this tight-binding model predicts that the electronic excitations can become more delocalized as |β| increases. Also note that, in an fcc close-packed 3D QD solid, the red shift should be ~24|β| as the number of nearest neighbors is 12.

The second picture is more localized. As the QDs are starved of capping molecules, the remaining capping molecules have more freedom to rearrange on each QD surface. This rearrangement may expose bare PbSe surfaces and allow the direct contact (without the intervening molecular layer) of neighboring quantum dots. Due to the high surface energy of the bare QD surface, we expect the direct contact or aggregation process to be thermodynamically favorable. This leads to a 2D network of strongly coupled QDs, resulting in exciton delocalization and a red shift in exciton energy. In fact, such a localized coupling mechanism is similar to those discovered by Kotov *et al.* for the nearly frustration-free formation of 1D nanowires or 2D nanosheets from the aggregation of QDs in the solution phase due to the slow and controlled removal of capping molecules.[22,23] In the present case on a 2D solid surface, the end result for the QD assemblies when all capping molecules are removed is similar to the delocalized mechanism in the previous paragraph. The difference lies in the extent of order/disorder: the delocalized coupling mechanism should yield a more ordered 2D superlattice, while the localized mechanism should give more disorder.

In reality, both localized and delocalized coupling mechanisms may operate to increase inter-QD electronic coupling. We arrive at two important conclusions regarding the strong inter-QD electronic coupling. First, the |β| value for 2D assemblies of PbSe QDs are as large as 7 and 13 meV (for 6 and 4 nm QDs), which is 1 order of magnitude larger than that for 3D solids with the same chemical treatment. We believe this is due to more significant geometric frustration in 3D assemblies than in 2D. Each QD in a 3D solid has 12 neighbors, as compared to 6 in the 2D assembly. The geometric frustration inhibits the close packing of QDs after the removal of the surface ligands. The large β value observed here for 2D PbSe assemblies is also consistent with a scanning tunneling microscopy and spectroscopy study of thermally annealed 2D assemblies of PbSe QDs by Liljeroth *et al.*[15] These authors performed calculations based on the effective mass model and showed that |β| could be as large as 25 meV for an inter-QD separation of 0.5 nm. Second, our results show that the inter-QD electronic coupling is continuously tunable for the 2D QD assemblies and that the coupling can be controlled simply by changing the hydrazine exposure time. Small changes in separation lead to large changes in the electronic coupling because the effective masses in PbSe are small. In other words, PbSe QDs have an increased spatial extension of the electron and hole wave functions outside the QD boundary. This leakage of the electron and hole will also increase with decreasing QD size. This is indeed observed experimentally: for 4 nm PbSe QDs the maximum |β| value is 13 meV while that for 6 nm QDs is 7 meV.

We now address the implications of the strong electronic coupling in QD solids on their applications, particularly photovoltaic devices. In a thin disordered film of PbSe QDs, depending on how the film was formed and treated, there may be domains of QDs with strong electronic coupling separated by boundaries where the coupling is weaker. These islands with strong electronic coupling may be viewed as "super" quantum dots where the electron and hole wave functions will be delocalized across the whole domain (island). We can identify at least four important roles that these strongly coupled domains can play in a photovoltaic device. First, the optical absorption cross section above the first exciton transition can increase with |β| such that the strongly coupled domains serve as enhanced light absorption centers. Second, energy transfer to the strongly coupled domains from the surrounding QDs can be a downhill process and serve as a pathway to channel excitation energy. These strongly coupled regions can act as basins for both charge and energy and influence how carriers and excitons move within the film. Charge transport in disordered QD solids occurs through strongly coupled percolation pathways or *via* hopping among these super dots or islands. Third, electronic delocalization within each strongly coupled domain decreases exciton binding energy and increases the probability of exciton dissociation. Fourth, electronic coupling and delocalization decrease the QD charging energy and increase charge mobility. One of the challenges in the design of future QD solar cells is to determine how to take advantage of these effects that arise due to strong electronic coupling. Another challenge is to find ways to assemble nanostructures that exploit such effects in order to increase the overall charge collection and power conversion efficiencies of these solar cells.

CONCLUSIONS

We find that hydrazine exposure of a two-dimensional PbSe QD array assembled on a solid sur-

face leads to strong and tunable electronic coupling, with β values as high as 13 meV. This is 1 order of magnitude greater than that previously achieved in 3D QD solids with the same chemical treatment. We attribute this much enhanced electronic coupling to reduced geometric frustration in 2D films. The ability to measure the coupling with such a simple technique will allow transport processes in QDs to be studied and understood more easily. This can lead to rational design of QD-based electronic and optoelectronic materials for solar cells and other applications.

METHODS

For our experiments, we synthesized PbSe QDs with average diameters (ϕ) between 4 and 6 nm (±5%) and surfaces capped with oleic acid.[19,26] All QD preparation and processing steps were carried out under an inert atmosphere in a glovebox. These nanocrystals were then placed on TiO_2 substrates for measurements. Specifically, rutile TiO_2 crystals with (110) surface orientation (Princeton Scientific) were cut and polished to the shape of a parallelogram (32 mm × 10 mm × 1 mm) with a 45° bevel on both ends. This allowed the substrate to be used as an ATR-FTIR waveguide. To obtain atomically flat TiO_2(110) surfaces, the crystal was immersed in 1 M HCl under ultraviolet illumination (254 nm) for 30 min, followed by rinsing with deionized water and acetone in air.[27] Each cleaned TiO_2 substrate was then transferred to the glovebox and, after a final rinse with distilled hexanes, dipped in the QD dispersion (1 mg/mL in hexane). The substrate was withdrawn at a rate of 1 cm/s for the deposition of QDs. Afterward, each sample was dried for 2 min. Hydrazine-treated samples were then submerged in a solution of 1 M hydrazine in acetonitrile and dried for an additional 2 min. We choose this hydrazine concentration following previous work of Nozik and co-workers who showed only removal of oleid-acid-capping molecules, without the change in QD size or the chemical reduction of PbSe; the latter occurred at much higher hydrazine concentrations.[18] ATR-FTIR spectroscopy measurements were carried out in the glovebox on a Nicolet 6700 FTIR-NIR spectrometer with an InGaAs detector. Atomic force microscopy was carried out on a humidity-controlled (≤5% RH) Agilent 5500 scanning probe microscope with a ~100 μm (*X*−*Y* range) scanner operated in open loop. A silicon tip integrated with a rectangular, uncoated silicon cantilever (Applied Nanostructures, <10 nm radius of curvature, 3 N/m nominal spring constant, resonance frequency of 67.30 kHz, and quality factor of ≈140) was used in AC mode so as to place the oscillator in the net attractive regime (diagnosed *via* the phase signal) at a drive frequency (67.53 kHz) above resonance and a set point amplitude of approximately 95% of the free oscillation amplitude (≈15 nm; *i.e.*, low kinetic energy, low tip−sample dissipation).[28] This minimal-perturbation configuration was generally needed for successful imaging to avoid capillary transfer of nanoparticles to the AFM tip, as readily occurred at ambient humidity and/or in a net repulsive regime (*i.e.*, "true tapping", achieved at higher free-oscillation amplitude, lower set point, or lower drive frequency).

Acknowledgment. This work was supported by the U.S. Department of Energy (DE-FG02-07ER46468) and utilized resources at the University of Minnesota Characterization Facility, funded by NSF through the NNIN program. Partial support from the NSF Nanoscale Interdisciplinary Research Team (NIRT) program (CBET-0506748) is also acknowledged.

REFERENCES AND NOTES

1. Murray, C. B.; Kagan, C. R.; Bawendi, M. G. Synthesis and Characterization of Monodisperse Nanocrystals and Close-Packed Nanocrystal Assemblies. *Annu. Rev. Mater. Sci.* **2000**, *30*, 545–610.
2. Murray, C. B.; Norris, D. J.; Bawendi, M. G. Synthesis and Characterization of Nearly Monodisperse CdE (E = Sulfur, Selenium, Tellurium) Semiconductor Nanocrystallites. *J. Am. Chem. Soc.* **1993**, *115*, 8706–8715.
3. Murray, C. B.; Kagan, C. R.; Bawendi, M. G. Self-Organization of CdSe Nanocrystallites into Three-Dimensional Quantum Dot Superlattices. *Science* **1995**, *270*, 1335–1338.
4. Shevchenko, E. V.; Talapin, D. V.; Kotov, N. A.; O'Brien, S.; Murray, C. B. Structural Diversity in Binary Nanoparticle Superlattices. *Nature* **2006**, *439*, 55–59.
5. Ginger, D. S.; Greenham, N. C. Charge Injection and Transport in Films of CdSe Nanocrystals. *J. Appl. Phys.* **2000**, *87*, 1361–1368.
6. Leatherdale, C. A.; Kagan, C. R.; Morgan, N. Y.; Empedocles, S. A.; Kastner, M.A.; Bawendi, M. G. Photoconductivity in CdSe Quantum Dot Solids. *Phys. Rev. B* **2000**, *62*, 2669–2680.
7. Morgan, N. Y.; Leatherdale, C. A.; Drndić, M.; Jarosz, M. V.; Kastner, M. A.; Bawendi, M. G. Electronic Transport in Films of Colloidal CdSe Nanocrystals. *Phys. Rev. B* **2002**, *66*, 075339.
8. Drndić, M.; Jarosz, M. V.; Morgan, N. Y.; Kastner, M. A.; Bawendi, M. G. Transport Properties of Annealed CdSe Colloidal Nanocrystal Solids. *J. Appl. Phys.* **2002**, *92*, 7498–7503.
9. Houtepen, A. J.; Kockmann, D.; Vanmaekelbergh, D. Reappraisal of Variable-Range Hopping in Quantum-Dot Solids. *Nano Lett.* **2008**, *8*, 3516–3520.
10. Mentzel, T. S.; Porter, V. J.; Geyer, S.; MacLean, K.; Bawendi, M. G.; Kastner, M. A. Charge Transport in PbSe Nanocrystal Arrays. *Phys. Rev. B* **2008**, *77*, 075316.
11. Artemyev, M. V.; Woggon, U.; Jaschinski, H.; Gurinovich, L. I.; Gaponenko, S. V. Spectroscopic Study of Electronic States in an Ensemble of Close-Packed CdSe Nanocrystals. *J. Phys. Chem. B* **2000**, *104*, 11617–11621.
12. Kim, D. I.; Islam, M. A.; Avila, L.; Herman, I. P. Contribution of the Loss of Nanocrystal Ligands to Interdot Coupling in Films of Small CdSe/1-Thioglycerol Nanocrystals. *J. Phys. Chem. B* **2003**, *107*, 6318–6323.
13. Warner, J. H. Self-Assembly of Ligand-Free PbS Nanocrystals into Nanorods and Their Nanosculpturing by Electron-Beam Irradiation. *Adv. Mater.* **2008**, *20*, 784–787.
14. Arachchige, I. U.; Brock, S. L. Sol−Gel Assembly of CdSe Nanoparticles to Form Porous Aerogel Networks. *J. Am. Chem. Soc.* **2006**, *128*, 7964–7971.
15. Liljeroth, P.; Overgaag, K.; Urbieta, A.; Grandidier, B.; Hickey, S. G.; Vanmaekelbergh, D. Variable Orbital Coupling in a Two-Dimensional Quantum-Dot Solid Probed on a Local Scale. *Phys. Rev. Lett.* **2006**, *97*, 096803.
16. Yu, D.; Wang, C.; Guyot-Sionnest, P. n-Type Conducting CdSe Nanocrystal Solids. *Science* **2003**, *300*, 1277–1280.
17. Talapin, D. V.; Murray, C. B. PbSe Nanocrystal Solids for N- and P-Channel Thin Film Field-Effect Transistors. *Science* **2005**, *310*, 86–89.
18. Law, M.; Luther, J. M.; Song, Q.; Hughes, B. K.; Perkins, C. J.; Nozik, A. J. Structural, Optical, and Electrical Properties of PbSe Nanocrystal Solids Treated Thermally or with Simple Amines. *J. Am. Chem. Soc.* **2008**, *130*, 5974–5985.
19. Luther, J. M.; Law, M.; Song, Q.; Perkins, C. J.; Beard, M. C.; Nozik, A. J. Structural, Optical, and Electrical Properties of Self-Assembled Films Of PbSe Nanocrystals Treated with 1,2-Ethanedithiol. *ACS Nano* **2008**, *2*, 271–280.
20. Luther, J. M.; Law, M.; Beard, M. C.; Song, Q.; Reese, M. O.; Ellingson, R. J.; Nozik, A. J. Schottky Solar Cells Based on Colloidal Nanocrystal Films. *Nano Lett.* **2008**, *8*, 3488–3492.
21. Koleilat, G. I.; Levina, L.; Shukla, H.; Myrskog, S. H.; Hinds, S.; Pattantyus-Abraham, G.; Sargent, E. H. Efficient, Stable Infrared Photovoltaics Based on Solution-Cast Colloidal Quantum Dots. *ACS Nano* **2008**, *2*, 833–840.

22. Tang, Z.; Kotov, N. A.; Giersig, M. Spontaneous Organization of Single CdTe Nanoparticles into Luminescent Nanowires. *Science* **2002**, *297*, 237–240.
23. Tang, Z.; Zhang, Z.; Wang, Y.; Glotzer, S. C.; Kotov, N. A. Self-Assembly of CdTe Nanocrystals into Free-Floating Sheets. *Science* **2006**, *314*, 274–278.
24. Wise, F. W. Lead Salt Quantum Dots: The Limit of Strong Quantum Confinement. *Acc. Chem. Res.* **2000**, *33*, 773–780.
25. Gersten, J. I.; Smith, F. W. *The Physics and Chemistry of Materials*; Wiley: New York, 2001; p 209.
26. Murphy, J. E.; Beard, M. C.; Nozik, A. J. Time-Resolved Photoconductivity of PbSe Nanocrystal Arrays. *J. Phys. Chem. B* **2006**, *110*, 25455–25461.
27. Lu, Y.; Jaeckel, B.; Parkinson, B. A. Preparation and Characterization of Terraced Surfaces of Low-Index Faces of Anatase, Rutile, and Brookite. *Langmuir* **2006**, *22*, 4472–4475.
28. Garcia, R; Perez, R. Dynamic Atomic Force Microscopy Methods. *Surf. Sci. Rep.* **2002**, *47*, 197–301.